Journal of Cardiovascular Magnetic Resonance 26 (2024) 101088

Contents lists available at ScienceDirect

Journal of Cardiovascular Magnetic Resonance

journal homepage: www.sciencedirect.com/journal/jocmr

Original Research

Impact of valve-sparing aortic root replacement on aortic fluid dynamics and biomechanics in patients with syndromic heritable thoracic aortic disease

Lydia Dux-Santoy[a,1], Aroa Ruiz-Muñoz[a,b,c,d,1], Andrea Guala[a,b,*], Laura Galian-Gay[b,c], Rubén Fernandez-Galera[c], Filipa Valente[c], Guillem Casas[c], Ruperto Oliveró[c], Marta Ferrer-Cornet[a], Mireia Bragulat-Arévalo[a,d], Alejandro Carrasco-Poves[a,d], Juan Garrido-Oliver[a,d], Alberto Morales-Galán[a], Kevin M. Johnson[f,g], Oliver Wieben[f,g], Ignacio Ferreira-González[a,c,d,e], Arturo Evangelista[a,b,c,d,h], Jose Rodriguez-Palomares[a,b,c,d,*], Gisela Teixidó-Turà[a,b,c]

[a] Vall d'Hebron Institut de Recerca (VHIR), Barcelona, Spain
[b] CIBER de Enfermedades Cardiovasculares, CIBER-CV, Instituto de Salud Carlos III, Madrid, Spain
[c] Department of Cardiology, Hospital Universitari Vall d'Hebron, Barcelona, Spain
[d] Department of Medicine, Universitat Autònoma de Barcelona, Bellaterra, Spain
[e] CIBER de Epidemiología y Salud Pública, CIBERESP, Instituto de Salud Carlos III, Madrid, Spain
[f] Department of Medical Physics, University of Wisconsin, Madison, Wisconsin, USA
[g] Department of Radiology, University of Wisconsin, Madison, Wisconsin, USA
[h] Instituto del Corazón, Quirónsalud-Teknon, Barcelona, Spain

ARTICLE INFO

Keywords:
Syndromic heritable thoracic aortic disease
Marfan syndrome
Loeys-Dietz syndrome
Valve-sparing aortic root replacement
4D flow CMR
Fluid dynamics

ABSTRACT

Background: Patients with syndromic heritable thoracic aortic diseases (sHTAD) who underwent prophylactic aortic root replacement are at high risk of distal aortic events, but the underlying mechanisms remain unclear. This prospective, longitudinal study evaluates the impact of valve-sparing aortic root replacement (VSARR) on aortic fluid dynamics and biomechanics in these patients.

Methods: Sixteen patients with Marfan or Loeys-Dietz syndrome underwent two time-resolved three-dimensional phase-contrast cardiovascular magnetic resonance (4D flow CMR) studies before (sHTAD-preSx) and after VSARR (sHTAD-postSx). Two matched cohorts of 40 healthy volunteers (HV) and 16 sHTAD patients without indication for aortic root replacement (sHTAD-NSx) with available 4D flow CMR were included for comparison. In-plane rotational flow (IRF), systolic flow reversal ratio (SFRR), wall shear stress (WSS), pulse wave velocity (PWV), and aortic strain were analyzed in the ascending (AscAo) and descending aorta (DescAo).

Results: All patients with sHTAD presented altered hemodynamics and increased stiffness ($p < 0.05$) compared to HV, both in the AscAo (median PWV 7.4 in sHTAD-NSx; 6.8 in sHTAD-preSx; 4.9 m/s in HV) and DescAo (median PWV 9.1 in sHTAD-NSx; 8.1 in sHTAD-preSx; 6.3 m/s in HV). Patients awaiting VSARR had markedly reduced in-plane (median IRF −2.2 vs 10.4 cm^2/s in HV, $p = 0.001$), but increased through-plane flow rotation (median SFRR 7.8 vs 3.8% in HV, $p = 0.002$), and decreased WSS (0.36 vs 0.47 N/m^2 in HV, $p = 0.004$) in the proximal DescAo. After VSARR, proximal DescAo IRF ($p = 0.010$) and circumferential WSS increased ($p = 0.011$), no longer differing from HV, but SFRR, axial WSS and stiffness remained altered. Patients in which aortic tortuosity was reduced after surgery showed greater post-surgical increase in IRF compared to those in

Abbreviations: 4D flow CMR, time-resolved three-dimensional phase-contrast cardiovascular magnetic resonance; AD, aortic distensibility; ARB, angiotensin receptor blocker; AscAo, ascending aorta; BSA, body surface area; CMR, cardiovascular magnetic resonance; DescAo, descending aorta; DBP, brachial diastolic blood pressure; HV, healthy volunteers; IRF, in-plane rotational flow; LDS, Loeys-Dietz syndrome; MFS, Marfan syndrome; NSx, no indication for aortic root replacement; preSx, prior to valve-sparing aortic root replacement; postSx, after undergoing valve-sparing aortic root replacement; PWV, pulse wave velocity; SBP, brachial systolic blood pressure; SFRR, systolic flow reversal ratio; sHTAD, syndromic heritable thoracic aortic disease; Sx, indication for valve-sparing aortic root replacement; VSARR, valve-sparing aortic root replacement; WSS, wall shear stress; PC-VIPR, phase contrast vastly undersampled isotropic projection

* Corresponding authors: Vall d'Hebron Institut de Recerca (VHIR) and Hospital Universitari Vall d'Hebron, Barcelona, Spain
E-mail addresses: andrea.guala@vhir.org (A. Guala), jfrodriguezpalomares@gmail.com (J. Rodriguez-Palomares).

[1] Lydia Dux-Santoy and Aroa Ruiz-Muñoz equally contributed to this work and are joint first authors.

https://doi.org/10.1016/j.jocmr.2024.101088
Received 5 February 2024; Received in revised form 8 August 2024; Accepted 21 August 2024

which tortuosity increased (median IRF increase 18.1 vs 3.3 cm^2/s, p = 0.047). Most AscAo flow alterations were restored to physiological values after VSARR.
Conclusion: In patients with sHTAD, VSARR partially restores downstream fluid dynamics to physiological levels. However, some flow disturbances and increased stiffness persist in the proximal DescAo. Further longitudinal studies are needed to evaluate whether persistent alterations contribute to post-surgical risk.

1. Introduction

Patients with syndromic heritable thoracic aortic diseases (sHTAD), such as Marfan (MFS) and Loeys-Dietz syndromes (LDS), frequently develop aortic root and ascending aorta (AscAo) aneurysms [1–3]. In cross-sectional and longitudinal studies of adults with MFS, more than 80% of the patients present aortic dilation during their lifetime [4,5]. Aortic dissection risk rises with aortic root diameters > 50 mm in MFS patients [6,7] and > 45 mm in LDS [2,8]. Imaging surveillance of the aorta and timely aortic root replacement prevent aortic events and death [9] and have dramatically improved life expectancy [10–12] in these patients. In recent years, valve-sparing aortic root replacement (VSARR) has become the standard of practice [9] with proven positive results [13–15].

While imaging and prophylactic aortic root replacement protect sHTAD patients from type A dissection, the risk of type B persists after intervention. Patients with MFS who have undergone aortic root replacement experience faster descending aorta (DescAo) dilation [16] and higher risk of later-onset type B dissection [17–19] than those without root replacement, even with slight DescAo dilation [17]. The underlying mechanisms for this increased risk remain unclear [16]. Two main hypotheses exist: one links risk to surgical trauma or graft-induced changes in aortic anatomy, fluid dynamics, and biomechanics [20], while the other holds that patients requiring surgery might present more aggressive vascular disease leading to the increased risk. Given this scenario, DescAo diameters are periodically monitored in sHTAD patients after aortic root replacement. However, as adverse events may also occur at lower diameters [2,8,9], there is a need for new imaging biomarkers for better risk assessment. For this reason, this study aimed (i) to assess the impact of VSARR in the aortic fluid dynamics and biomechanics of sHTAD patients and their relationship with changes in aortic geometry after surgery, and (ii) to evaluate aortic flow and biomechanics at different stages of the aortic disease by comparing patients awaiting aortic root surgery with patients with no indication for aortic root surgery and healthy volunteers (HV).

2. Methods

2.1. Study design and population

Adult patients (> 18 years) with genetically confirmed sHTAD (MFS or LDS), followed at the Genetic Aortic Unit of Vall d'Hebron Hospital, and meeting criteria for elective VSARR were prospectively invited to participate in this study. Patients with previous aortic dissection or surgery, or contraindication for cardiovascular magnetic resonance (CMR) were excluded. Patients accepting to participate formed the surgical cohort named sHTAD-Sx and were scheduled for two CMR studies: one before (< 12 months, sHTAD-preSx) and another after (> 3 months, sHTAD-postSx) the intervention.

Two further cohorts of subjects with previously available time-resolved three-dimensional phase-contrast cardiovascular magnetic resonance (4D flow CMR) [21] were retrospectively identified and included for comparison (Fig. 1): (i) a cohort of HVs matched for age, sex, and body surface area (BSA); and (ii) a cohort of genetically-confirmed sHTAD patients without indication for aortic root replacement (sHTAD-NSx), no previous dissection or surgery, and matched for age, sex, BSA, DescAo diameter, and type of genetic syndrome (MFS or LDS). Of note, patients identified for the sHTAD-NSx cohort did not meet surgical criteria during the 4.2 [3.7–6.5] years (median [interquartile range]) passed after the CMR study, confirming their benign profile. The degree of aortic valve regurgitation and aortic valve peak velocity were

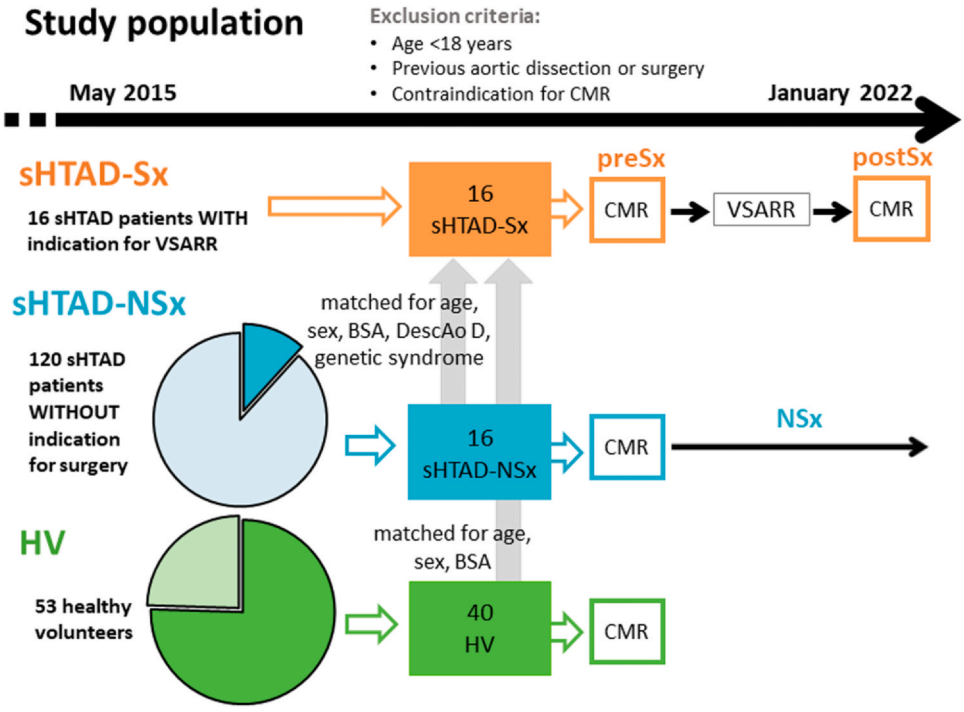

Fig. 1. Flowchart of patient inclusion. sHTAD patients with indication for VSARR underwent preSx and postSx CMR and were compared with matched cohorts of sHTAD not meeting surgical criteria and HV to assess the impact of VSARR. *CMR* cardiovascular magnetic resonance, *sHTAD* syndromic heritable thoracic aortic disease, *Sx* indication for valve-sparing aortic root replacement, *VSARR* valve-sparing aortic root replacement, *preSx* prior to valve-sparing aortic root replacement, *postSx* after undergoing valve-sparing aortic root replacement, *BSA* body surface area, *DescAo* descending aorta, *NSx* no indication for aortic root replacement, *HV* healthy volunteers

retrieved from clinical echocardiography studies acquired near to each CMR study. Additionally, previous growth rates during follow-up were computed from echocardiographic measurements in sHTAD-NSx and sHTAD-preSx. The study was approved by the institutional ethics committee (PR(AG)23/2018 on February 16, 2018) and written informed consent was obtained from all participants.

2.2. Cardiovascular magnetic resonance protocol

CMR studies were performed on a clinical 1.5T MRI scanner (Signa, GE HealthCare, Waukesha, Wisconsin). The protocol included double-oblique balanced steady-state free-precession cine images to evaluate AscAo and DescAo diameters and distensibility, and AscAo longitudinal strain; and a 4D flow CMR study to analyze aortic flow dynamics, pulse wave velocity (PWV) and geometry.

A phase-contrast vastly undersampled isotropic projection (PC-VIPR) acquisition with 5-point balanced velocity encoding [22] and retrospective electrocardiogram gating during free-breathing was used for 4D flow CMR of the entire thoracic aorta. 4D flow CMR studies were acquired using the following parameters: velocity encoding determined according to maximum velocity at the aortic valve (from 150 to 200 cm/s), field of view 400 × 400 × 400 mm, acquisition matrix 160 × 160 × 160, voxel size 2.5 × 2.5 × 2.5 mm, and flip angle 8°. The dataset was reconstructed according to the nominal temporal resolution (5 × TR) of each patient (21–42 ms). Data were corrected for background phase from concomitant gradients, eddy currents, and trajectory errors [22].

Cine images had a homogeneous in-plane spatial resolution between 1.56 and 1.88 mm, and 30 phases during the cardiac cycle were obtained, which permits reliable computation of distensibility [23].

Brachial systolic and diastolic blood pressures were taken immediately after the CMR study.

2.3. Aortic flow dynamics evaluation with 4D flow CMR

Using the phase-contrast enhanced angiogram derived from the 4D flow CMR, several anatomical landmarks were manually located and the thoracic aorta was semi-automatically segmented [24]. Twenty-four equidistant planes perpendicular to the aortic centreline were located: eight in the AscAo (from the sinotubular junction to the innominate artery), four in the arch (from the innominate artery to the left subclavian artery), eight in the proximal (from the left subclavian artery to the level of the pulmonary artery bifurcation), and four in the distal DescAo (from the level of the pulmonary artery bifurcation to the diaphragmatic level).

The three-dimensional (3D) aortic segmentations were used to extract the velocity data inside the aorta. Different flow parameters were computed in each analysis plane using custom-designed MATLAB code (MathWorks, Natick, Massachusetts, USA), as described [25,26]:

- Maximum velocity.
- Peak-systolic in-plane rotational flow (IRF), which evaluates flow rotation within a plane, was computed as the through-plane component of circulation, defined as the integral of vorticity with respect to the cross-sectional area.
- Systolic flow reversal ratio (SFRR), which quantifies through-plane vortexes as relative amount of backward flow in systole, was obtained as the ratio of backward (V_{SBF}) to forward (V_{SFF}) through-plane systolic volumes, $SFRR(\%) = \frac{V_{SBF}}{V_{SFF}} \cdot 100$.
- Peak-systolic wall shear stress (WSS) was obtained by fitting the 3D velocity data with B-spline surfaces and computing velocity derivatives on the segmented aortic contour at each plane [27]. It was decomposed into axial and circumferential components.

All peak-systolic parameters were averaged using one time-frame before and two time-frames after peak systole to mitigate noise [25].

Visualization of systolic streamlines was performed in Paraview 5.10 (Kitware Inc., Clifton Park, New York, USA), after processing 4D flow acquisitions [28].

2.4. Aortic mechanical properties

Aortic biomechanics were characterized by means of regional aortic PWV, aortic distensibility (AD), and longitudinal strain.

AscAo and DescAo PWV were computed from 4D flow CMR as described [29,30]. The transit time between velocity waveforms was computed with a wavelet-based method, the most robust technique [31].

AD was calculated from double-oblique cine imaging in the AscAo and DescAo at the pulmonary artery level [30]. Using ARTFUN software (Inserm U678, Paris, France), maximum (A_{max}) and minimum (A_{min}) aortic area were obtained from semi-automatically traced aortic contours and used to compute AD as shown in Fig. 2.

Proximal AscAo longitudinal strain was computed by tracking the aortic valve throughout the cardiac cycle from a set of coronal, sagittal, and aortic valve cine images using in-house code [32]. The 3D valve movement was projected in the direction of the aortic centreline to measure the maximum longitudinal displacement of the valve. Longitudinal strain was obtained as the ratio between maximum displacement and AscAo length (Fig. 2).

All these biomarkers were previously validated against destructive mechanical testing on ex-vivo aortic specimens [29].

2.5. Aortic geometry

Using cine CMR acquisition, end-diastolic diameters were measured. In the aortic root, the three cusp-to-cusp diameters were quantified and its maximum was retained for the analysis. AscAo and DescAo diameters were assessed at the level of the pulmonary artery. Moreover, at each analysis plane, local aortic diameter was automatically extracted from the segmentation.

The length of the AscAo was measured from the sinotubular junction to the first supra-aortic vessel using the aortic centreline. AscAo-arch tortuosity was defined as the length of the centreline from the sinotubular junction to the DescAo at the level of the pulmonary bifurcation divided by the linear distance between these points, as is commonly done [33].

2.6. Statistical analysis

Continuous variables are expressed as median [first–third] quartiles. Categorical variables are presented as frequency (percentage). Distribution normality was assessed by the Shapiro-Wilk test. Differences among groups for continuous parameters were assessed by Student's t-test if normally distributed and Mann-Whitney U test otherwise, while chi-square test was used for categorical variables. Differences between paired samples were assessed by the Wilcoxon signed-rank statistic test for continuous variables and McNemar's test for categorical variables. The association of post- and pre-surgical differences of flow and biomechanical parameters with those of geometrical parameters were assessed using Spearman correlation (ρ) or Mann-Whitney U test when comparing groups. A two-tailed p-value < 0.05 was considered statistically significant. SPSS 21.0 (IBM, SPSS Statistics, Chicago, Illinois, USA) was used.

3. Results

3.1. Demographic and clinical data

The study cohort included 16 patients with sHTAD (13 with MFS, 3 with LDS) referred for VSARR in the sHTAD-Sx group, 16 patients with sHTAD (12 MFS, 4 LDS) and no indication for VSARR in the sHTAD-NSx

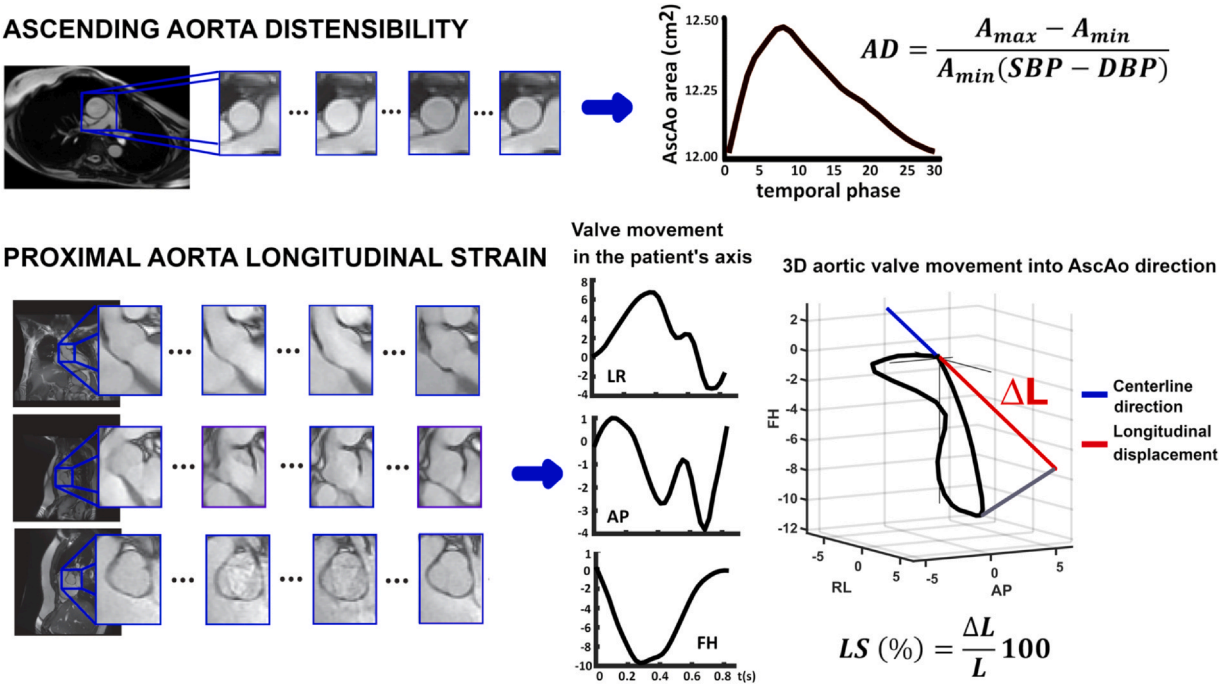

Fig. 2. Ascending aorta distensibility (top) and longitudinal strain (bottom) quantification. Ascending aorta distensibility was computed at the level of the pulmonary artery bifurcation, from temporal evolution of the cross-sectional area in cine CMR. Longitudinal strain was obtained by tracking the aortic valve movement on sagittal, coronal, and aortic valve cine images. The three-dimensional displacement of the valve is obtained and averaged in the patient's axis (*LR* left-right, *AP* anterior-posterior, *FH* feet-head) and then projected in the direction of the proximal aorta centreline. *AD* aortic distensibility, A_{max} maximum aortic area, A_{min} minimum aortic area, *SBP* brachial systolic blood pressure, *DBP* diastolic blood pressure, *3D* three-dimensional, *AscAo* ascending aorta

group, and 40 HV. In sHTAD-Sx, the preSx CMR was acquired 3.5 [1.2–8.4] months before VSARR, while the postSx CMR was acquired 8.1 [6.1–15.1] months after surgery. The demographic and clinical characteristics of these cohorts are shown in Table 1.

Compared to HV, patients with sHTAD were taller and had larger stroke volume and aortic diameters, irrespectively of the indication for surgery. Compared to sHTAD-NSx patients, sHTAD-preSx had larger left ventricular end-systolic, end-diastolic, and stroke volumes and larger aortic root and AscAo diameters, along with a tendency to faster aortic root dilation in the last 3.1 [2.8–3.3] years. The degree of aortic regurgitation was ≤II in all patients with sHTAD and no patient had aortic stenosis. Compared to data before the intervention, sHTAD-Sx presented increased aortic valve peak velocity after surgery and higher heart rate during the postsurgical CMR.

3.2. Fluid dynamics and biomechanics at different stages of aortic root disease

Flow dynamics and aortic stiffness parameters in the different groups are presented in Fig. 3 and Table 2, respectively. Flow dynamics for each analysis plane are detailed in Supplementary Tables S1-S5. Patients with sHTAD, irrespectively of meeting surgical criteria or not, presented altered aortic flow dynamics compared to HV, but these alterations were more pronounced in sHTAD-preSx patients (Fig. 3). Compared to HV, sHTAD-NSx patients presented slightly increased IRF (Fig. 3B) and decreased axial WSS (Fig. 3D) at the most proximal AscAo. Conversely, sHTAD-preSx patients showed a marked increase in all flow rotation descriptors (Fig. 3B, C, and E) and reduced axial WSS in the most proximal AscAo (Fig. 3D), as well as lower maximum velocity along the AscAo (Fig. 3A).

Altered flow dynamics were also noted in the aortic arch and proximal DescAo in all sHTAD patients. Compared to HV, DescAo IRF, and circumferential WSS were slightly reduced in sHTAD-NSx and markedly reduced in sHTAD-preSx (Fig. 3B and E). Moreover, sHTAD-preSx patients further presented markedly increased SFRR and decreased axial WSS at the proximal DescAo (Fig. 3C and D), both not seen in sHTAD-NSx.

Regarding aortic biomechanics (Table 2), both sHTAD-NSx and sHTAD-Sx patients had stiffer aortas than HV, measured as higher AscAo and DescAo PWV and lower AscAo AD, while AscAo longitudinal strain was similar. However, no difference in stiffness was found between sHTAD-Sx and sHTAD-NSx.

3.3. Impact of valve-sparing aortic root replacement

Regional flow dynamic and biomechanical parameters in patients before and after undergoing VSARR, and HVs are shown in Fig. 4 and Table 2. In Fig. 5, peak systolic streamlines are shown for several patients before and after VSARR. Certain pre-surgical flow abnormalities were restored after surgery, while others persisted altered. Specifically, regarding AscAo fluid dynamics, sHTAD-Sx patients showed increased maximum velocity (Fig. 5B, left and middle) and axial WSS and decreased proximal AscAo SFRR in the sHTAD-postSx compared to the sHTAD-preSx study (Fig. 4A, C, and D). With the exception of axial WSS, these AscAo flow parameters were indeed restored by VSARR, resulting in values no longer different from those seen in HV. Of note, differences between post- and pre-surgical proximal AscAo SFRR and axial WSS were related to changes in the average proximal aorta diameter ($\rho = 0.835$, $p < 0.0001$; $\rho = -0.700$, $p = 0.003$, respectively).

Regarding the arch and DescAo, VSARR markedly increased IRF and circumferential WSS (Fig. 5, middle and right), thereby partially restoring them to values observed in HV (Fig. 4B and F). Differences in IRF and circumferential WSS between sHTAD-postSx and sHTAD-preSx were mainly observed at the distal arch and the very proximal DescAo. Patients in which AscAo-arch tortuosity was reduced after surgery (69%, 11 out of 16 patients), presented larger post-surgical increase in IRF compared to patients in which tortuosity increased (median IRF increase 18.1 [4.2–37.1] vs 3.3 [−20.2 to 15.0] cm^2/s, $p = 0.047$). In contrast, the high values of SFRR at the proximal DescAo (Fig. 4C), and the low values of axial WSS along the entire thoracic aorta (Fig. 4D)

Table 1
Demographics and clinical data of the included cohorts.

	HV N = 40	sHTAD-NSx N = 16	sHTAD-Sx N = 16		NSx vs HV	preSx vs HV	preSx vs NSx	preSx vs postSx
			preSx	postSx	p-value	p-value	p-value	p-value
Genetic syndrome								
Marfan	NA	12 (75%)	13 (81%)		NA	NA	0.669	NA
Loeys-Dietz		4 (25%)	3 (19%)					
Age (years)	35 [30–45]	32 [24–45]	31 [25–42]	32 [28–45]	0.314	0.301	0.985	**0.002**
Male (N (%))	25 (62%)	10 (62%)	10 (62%)		1.000	1.000	1.000	NA
Weight (kg)	70 [62–80]	70 [64–82]	69 [58–82]	69 [59–85]	0.548	0.839	0.763	0.055
Height (cm)	173 [163–176]	180 [175–184]	185 [174–190]	184 [174–189]	**0.004**	**0.002**	0.428	0.394
BSA (m^2)	1.8 [1.7–1.9]	1.9 [1.8–2.1]	1.9 [1.7–2.1]	1.9 [1.8–2.1]	0.161	0.150	0.910	0.116
SBP (mm Hg)	120 [110–130]	115 [107–141]	119 [110–136]	123 [113–140]	0.642	0.933	0.737	0.263
DBP (mm Hg)	70 [60–77]	79 [62–82]	70 [62–79]	74 [69–81]	0.188	0.609	0.501	0.401
Stroke volume (mL)	84 [68–93]	95 [87–129]	126 [107–141]	106 [95–120]	**0.014**	< **0.001**	**0.015**	0.155
LV ejection fraction (%)	62 [58–66]	67 [62–67]	64 [59–67]	62 [55–69]	**0.029**	0.717	0.134	0.272
EDV (mL)	138 [117–148]	141 [133–189]	212 [162–226]	173 [156–215]	0.105	< **0.001**	**0.005**	0.272
ESV (mL)	52 [43–60]	56 [42–66]	72 [58–93]	70 [54–89]	0.528	< **0.001**	**0.007**	0.480
HR (bpm)	62 [56–66]	51 [44–56]	57 [49–65]	65 [58–71]	0.322	0.142	0.098	**0.011**
Aortic root diameter (mm)	27 [26–32]	37 [35–41]	49 [48–52]	25 [23–26]	< **0.001**	< **0.001**	< **0.001**	**0.003**
AscAo diameter (mm)	26 [23–28]	28 [25–31]	33 [30–36]	28 [28–30]	**0.052**	< **0.001**	**0.016**	**0.016**
DescAo diameter (mm)	19 [18–22]	22 [20–25]	23 [20–25]	23 [21–25]	**0.002**	**0.002**	0.985	0.889
AscAo-arch tortuosity	2.2 [2.1–2.4]	2.3 [2.1–2.6]	2.3 [2.1–2.6]	2.3 [2.1–2.4]	0.238	0.231	0.851	0.535
AscAo length (mm)	74 [61–85]	89 [80–105]	97 [81–105]	92 [80–100]	**0.002**	< **0.001**	0.572	0.679
Aortic root growth rate (mm/y)	NA	0.33 [0.00–1.26]	1.16 [0.38–2.10]	NA	NA	NA	0.063	NA
Treatment								
No treatment	40 (100%)	4 (31%)	2 (12%)	3 (19%)				
ARB	0	5 (38%)	11 (69%)	9 (56%)	NA	NA	0.302	0.564
Beta blocker	0	3 (23%)	3 (19%)	3 (19%)				
ARB + beta blocker	0	1 (8%)	0 (0%)	1 (6%)				
Aortic valve peak velocity (m/s)	NA	1.1 [1.0–1.2]	1.0 [0.9–1.2]	1.33 [1.02–1.60]	NA	NA	0.219	**0.022**
Aortic regurgitation								
0	NA	13 (81%)	8 (50%)	7 (44%)	NA	NA	0.635	0.566
I		2 (12%)	4 (25%)	7 (44%)				
II		1 (1%)	4 (25%)	2 (12%)				

Values are median [first; third interquartile] or n (%). p-values refer to bivariate analyses. Bold numbers indicate significant differences between the groups
ARB angiotensin receptor blocker, *HR* heart rate, *LV* left ventricular, *EDV* end-diastolic volume, *ESV* end-systolic volume, *NA* not applicable, *HV* healthy volunteers, *sHTAD* syndromic heritable thoracic aortic disease, *NSx* no indication for aortic root replacement, *Sx* indication for valve-sparing aortic root replacement, *preSx* prior to valve-sparing aortic root replacement, *postSx* after undergoing valve-sparing aortic root replacement, *BSA* body surface area, *SBP*0 *DBP* brachial diastolic blood pressure, *AscAo* ascending aorta, *DescAo* descending aorta

observed prior to VSARR persisted after surgery. Indeed, DescAo SFRR was slightly higher after surgery compared to pre-surgical values, but this change did not reach statistical significance.

AscAo longitudinal strain was reduced after surgery. DescAo stiffness was comparable before and after VSARR, thus maintaining all pre-existing differences in DescAo PWV and AD compared to HV (Table 2).

4. Discussion

This study describes the impact of elective prophylactic VSARR on the aortic fluid dynamics and biomechanics in patients with sHTAD, including MFS and LDS. Moreover, it deepens the knowledge of the relationship between different stages of the aortic root dilation in these patients and their aortic fluid dynamics and biomechanics by comparing sHTAD patients awaiting VSARR with properly matched cohorts of sHTAD patients without criteria for aortic surgery (neither in the present nor during a median follow-up of 4.2 years) and HV. The results of this work show that VSARR partially restores aortic flow to physiological values obtained in healthy subjects and has no short-term impact on aortic biomechanics in patients with sHTAD, thus suggesting that VSARR has no deleterious effects in the aortic arch and proximal DescAo fluid dynamics and biomechanics.

To the best of authors' knowledge, this is the first study analyzing the impact of VSARR on downstream aortic fluid dynamics and biomechanics in Marfan and Loeys-Dietz. Previous studies have included small heterogeneous cohorts with different aneurysm etiologies [20,34] or have focused on the effect of different types of intervention (VSARR, Bentall procedure, and aortic valve replacement) [35–38]. Moreover, most studies compared flow patterns of operated patients with HVs [35,37,38] or matched cohorts of pre-surgical patients [34], but not pre- and post-surgical flow in the same patients. Furthermore, in contrast to the present study, previous research [34,35,38] did not quantitatively evaluate rotational flow parameters with potential clinical significance [26]. Of note, a previous post-VSARR follow-up study in patients with MFS found altered flow dynamics to be potentially linked to type B dissection [39].

All patients with sHTAD included in this study presented with altered flow and WSS in the whole thoracic aorta compared to HV, but these disturbances were more pronounced in patients meeting criteria for elective prophylactic VSARR, who also experienced faster growth in the last 3 years. This highlights a rather logical dose-response, where larger aneurysms result in lower local blood velocity, which propagates via inertial effect through the distal AscAo and impacts DescAo flow characteristics [40,41]. In the DescAo, this was mainly visible in parameters describing both in-plane (IRF and circumferential WSS) and through-plane (SFRR) flow rotation, even in absence of local dilation. Indeed, in sHTAD-NSx patients, these flow descriptors presented intermediate-stage alterations with parameter values between HV and sHTAD-preSx patients. Of note, rotational flow variables have been previously suggested as early markers of DescAo dilation in patients with MFS [26].

After VSARR, some of the flow disturbances were partially restored, while others were unchanged, especially at the DescAo. In the AscAo, local change in diameter was related to changes in maximum velocity and proximal AscAo SFRR. Moreover, in the DescAo, IRF and circumferential WSS were increased and partially restored to physiological values observed in HV, while the increased SFRR and reduced axial WSS were maintained. Of note, surgery-related reduction of tortuosity

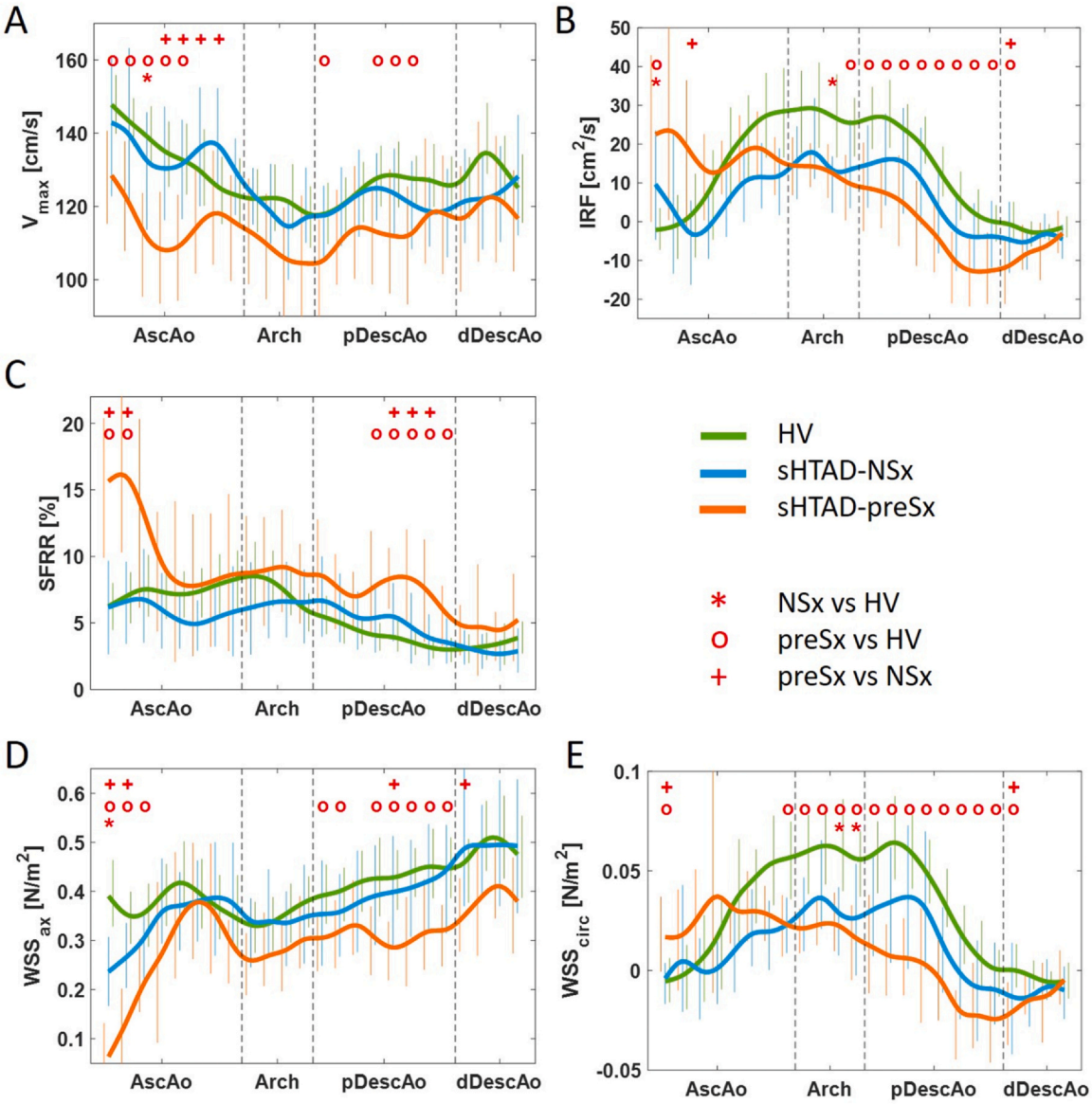

Fig. 3. Flow dynamics along the thoracic aorta in sHTAD patients with (preSx) and without (NSx) indication for VSARR and in healthy volunteers. (A) Maximum velocity, (B) IRF, (C) SFRR, and (D) axial and (E) circumferential WSS. Lines are colored green for HV, blue for sHTAD-NSx, and orange for sHTAD-preSx. Symbols *, o, and + indicate statistically significant differences ($p < 0.05$) between sHTAD-NSx and HV, sHTAD-preSx and HV, and preSx and NSx, respectively. *HV* healthy volunteers, *sHTAD* syndromic heritable thoracic aortic disease, *NSx* no indication for aortic root replacement, *preSx* prior to valve-sparing aortic root replacement, *AscAo* ascending aorta, *DescAo* descending aorta, *IRF* in-plane rotational flow, *SFRR* systolic flow reversal ratio, *WSS* wall shear stress, *pDescAo* proximal DescAo, *dDescAo* distal DescAo, *VSARR* valve-sparing aortic root replacement

was related to a more marked restauration of IRF at the DescAo. In line with these results, a previous study including patients with heritable aortic diseases of different aetiologies found that WSS in the DescAo was increased after AscAo graft replacement (81%, 13 out of 16 patients, with VSARR) [20]. Nonetheless, in that study, the authors suggested that the increase in WSS was a negative consequence of the surgery, although no comparison with physiological values in HV was provided. In contrast, the present results suggest that the post-surgical increase of circumferential WSS might be positive, since its values after surgery are more similar to those in HV. Different results have been reported in patients with bicuspid and tricuspid aortic valves, in which DescAo helical flow was found to be similar before and after VSARR [34,42]. Another small study reported that non-genetic patients presented increased pre-surgical DescAo WSS compared to matched controls with aortopathy not meeting surgical criteria, which was normalized after intervention (only 4 patients with VSARR and 2 with VSARR and hemiarch replacement out of 33) [36].

Data from the present work revealed that the severely increased proximal AscAo SFRR in sHTAD patients awaiting VSARR was completely restored after surgery, while axial WSS persisted and slightly reduced. These changes were related to the surgical reduction of aortic root and AscAo diameters. The present data concur with previous cross-sectional studies reporting that AscAo helical flow was reduced in patients with tricuspid and bicuspid aortic valves after VSARR compared to a well-matched pre-surgical cohort [34] and was similar to HV [42]. It is worth noting that in patients with those aortic conditions AscAo rotational flow was also recovered after Bentall with mechanical valve and VSARR procedures [42,43]. On the other hand, similar to the present results, AscAo WSS was observed to increase in patients with heritable aortic diseases of different aetiologies undergoing AscAo graft replacement [20].

Regarding aortic biomechanics, this work consistently shows that all sHTAD patients have stiffer AscAo and DescAo compared to HV, independently of meeting surgical criteria or not, and that VSARR does

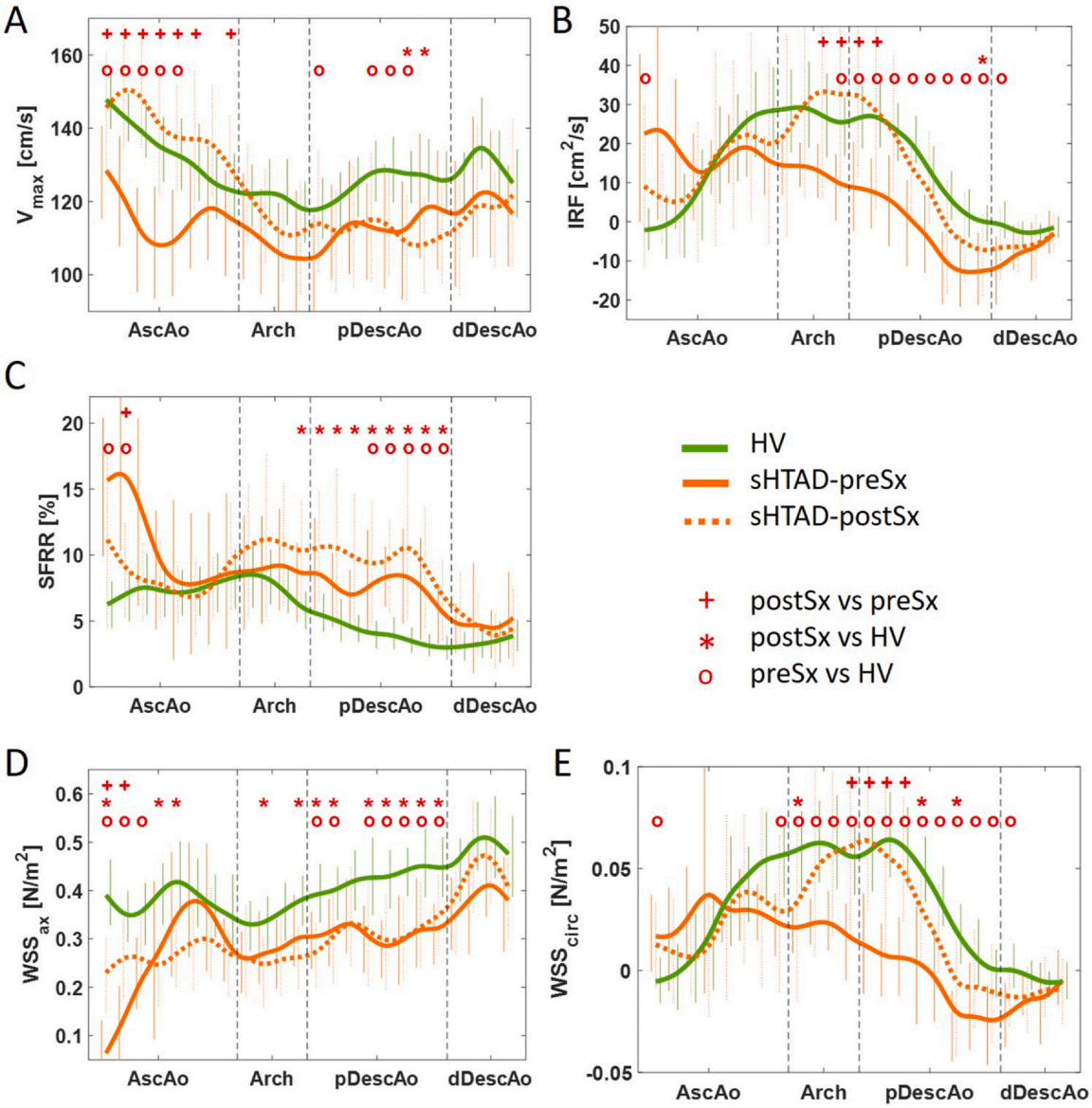

Fig. 4. Flow dynamics along the thoracic aorta in sHTAD patients undergoing VSARR before (preSx) and after (postSx) surgery, and in healthy volunteers. (A) Maximum velocity, (B) IRF, (C) SFRR, and (D) axial and (E) circumferential WSS. Lines are colored green for HV, orange for sHTAD patients, continuous for sHTAD-preSx, and dotted for sHTAD-postSx. Symbols o, *, and + indicate statistically significant differences ($p < 0.05$) between sHTAD-preSx and HV, sHTAD-postSx, and sHTAD-postSx and sHTAD-preSx, respectively. *HV* healthy volunteers, *sHTAD* syndromic heritable thoracic aortic disease, *preSx* prior to valve-sparing aortic root replacement, *postSx* after undergoing valve-sparing aortic root replacement, *AscAo* ascending aorta, *DescAo* descending aorta, *IRF* in-plane rotational flow, *SFRR* systolic flow reversal ratio, *WSS* wall shear stress, *pDescAo* proximal DescAo, *dDescAo* distal DescAo, *VSARR* valve-sparing aortic root replacement

Table 2
Aortic biomechanics of the included cohorts.

	HV N = 40	sHTAD-NSx N = 16	sHTAD-Sx N = 16		NSx vs HV	preSx vs HV	preSx vs NSx	preSx vs postSx
			preSx	postSx	p-value	p-value	p-value	p-value
AscAo PWV (m/s)	4.9 [4.1–6.2]	7.4 [6.0–8.5]	6.8 [4.2–8.0]	NA	**0.001**	**0.046**	0.280	NA
DescAo PWV (m/s)	6.3 [5.0–8.5]	9.1 [7.3–13.8]	8.1 [6.1–11.5]	9.1 [7.5–11.5]	**0.001**	**0.019**	0.533	0.875
AscAo AD ($mm\,Hg^{-1}\,10^{-3}$)	5.6 [3.8–6.6]	2.5 [1.8–4.8]	2.4 [1.5–4.9]	NA	**0.007**	**0.009**	0.872	NA
DescAo AD ($mm\,Hg^{-1}\,10^{-3}$)	4.5 [3.6–5.3]	3.5 [2.2–5.3]	3.3 [2.5–4.2]	2.4 [1.9–3.3]	0.178	**0.049**	0.794	0.260
AscAo longitudinal strain (%)	14.4 [10.3–16.6]	12.3 [9.0–17.1]	11.6 [8.2–13.8]	7.3 [5.7–11.1]	0.598	0.106	0.600	**0.013**

Values are median [first; third interquartile]. p-values refer to bivariate analyses. Bold numbers indicate significant differences between the groups
HV healthy volunteers, *sHTAD* syndromic heritable thoracic aortic disease, *NSx* no indication for aortic root replacement, *Sx* indication for valve-sparing aortic root replacement, *preSx* prior to valve-sparing aortic root replacement, *postSx after* undergoing valve-sparing aortic root replacement, *AscAo* ascending aorta, *DescAo* descending aorta, *PWV* pulse wave velocity, *AD* aortic distensibility

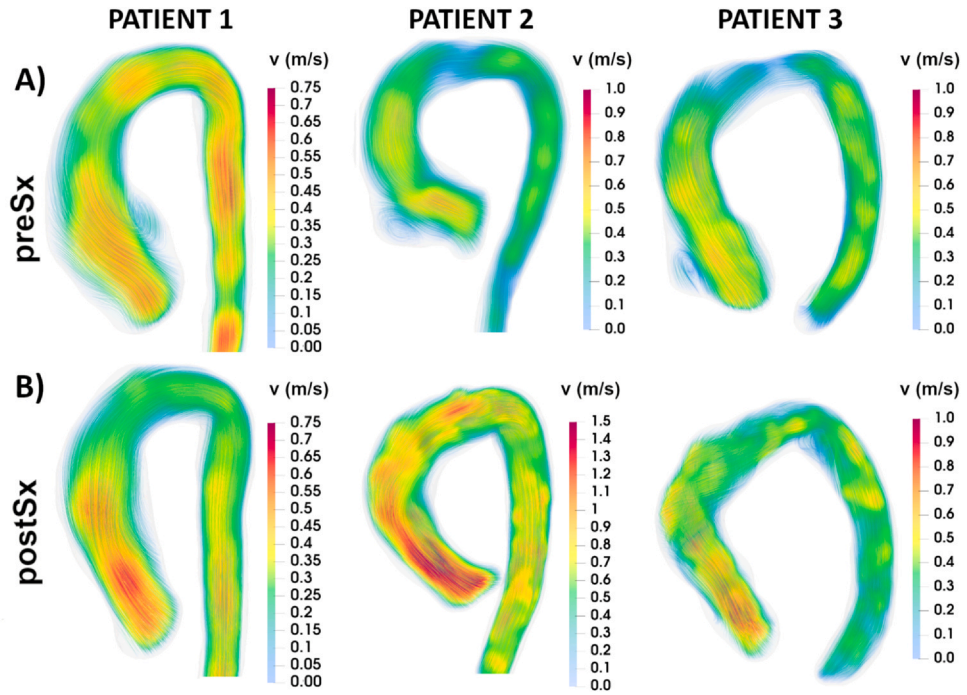

Fig. 5. Systolic velocity streamlines in three patients with Marfan syndrome before (A) and after (B) undergoing valve-sparing aortic root replacement (VSARR). Increased velocity in the ascending aorta after VSARR is shown in all patients. Increased rotational flow from the distal ascending aorta is observed in patients 2 and 3. Vortical flow after VSARR is visible in the proximal-inner descending aorta in patient 3. *preSx* prior to valve-sparing aortic root replacement, *postSx* after undergoing valve-sparing aortic root replacement

not have any short-term impact on DescAo stiffness. This result concurs with a previous study reporting similar carotid-femoral PWV before and after prosthetic replacement of the AscAo and the aortic root [44]. However, other studies reported that native DescAo stiffness (circumferential strain, fractional area changes, or AD), assessed by CMR [20] or echocardiography [45], was decreased after prosthetic AscAo replacement in patients with congenital or genetic conditions (including but not limited to sHTAD). The heterogeneous surgical procedures and cohorts included in those studies may explain these discrepancies.

Prior studies have associated previous prophylactic aortic root repair with faster DescAo dilation and an increased risk of type B aortic dissection in MFS patients [17–19], but the underlying mechanisms are not well understood. It has been suggested that this higher risk might be related to anatomical, fluid dynamic, and biomechanical changes induced by the surgery [20]. In light of the present work, VSARR itself does not have deleterious effects on downstream aortic flow dynamics and biomechanics in sHTAD patients, as flow dynamics are partially restored to physiological values found in healthy subjects, while biomechanics were unaltered. However, the extent of backward systolic flow and thus through-plane vortexes, here measured by SFRR, were related to the severity of aortic root disease and were not recovered by the intervention. As that, this flow abnormality might evidence the local impact of the severity of the aortopathy and might be responsible for the relative increase in risk of DescAo events and fast growth in patients with severe aortic root dilation, irrespectively of previous VSARR. The persistence of vortical flow in the proximal DescAo after VSARR is a plausible risk factor for later aortic events [39]. Further investigation is warranted to determine whether these abnormalities may hold a causative association with the risk for later-onset type B dissection.

5. Limitations

When considering the present findings, certain study limitations should be considered. The size of the cohort is modest, which is partially due to the low prevalence of MFS and LDS. However, it is worth noting that this is the first work assessing pre- and post-surgical fluid dynamics and biomechanics in selected patients with confirmed sHTAD undergoing VSARR. As post-surgical changes were assessed 8.1 [3.9–23.0] months after surgery, this study does not assess possible long-term post-surgical changes. Considering the relatively low number of subjects included, it was not possible to analyze aortic fluid dynamics and biomechanics separately for each gene variant or type of medical treatment. Finally, geometrical analysis was limited to basic descriptors. A more in-depth geometrical assessment with multimodality imaging could provide further details on the local relationships between altered flow dynamics and subsequent risk [46].

6. Conclusions

Patients with sHTAD awaiting prophylactic surgery of the proximal aorta present more pronounced flow disturbances along the whole thoracic aorta compared to patients at earlier stage of aortic disease. VSARR restores certain AscAo and DescAo fluid variables to physiological values obtained in healthy subjects. However, reduced axial WSS and increased vortical flow and stiffness persist altered at the DescAo. Further longitudinal studies are needed to elucidate whether the non-restored flow alterations at the DescAo may contribute to the risk of post-surgical aortic events.

Funding

This study has been supported by funding from the Instituto de Salud Carlos III (projects PI17/00381, PI20/01727, and PI21/00448), the Spanish Ministry of Science, Innovation and Universities (FORT23/00034, RTC2019-007280-1), the Spanish Society of Cardiology (SEC/FEC-INV-CLI 20/015, SEC/FEC-INV-CLI 21/030, and SEC/FEC-INV-CLI 23/08), and the Biomedical Research Networking Center on Cardiovascular Diseases (CIBERCV). Andrea Guala has received funding from “la Caixa” Foundation (LCF/BQ/PR22/11920008). Juan Garrido-Oliver has received funding from Secretaria d'Universitats i Recerca del Departament de Recerca i Universitats de la Generalitat de Catalunya i del Fons Europeu Social Plus (AGAUR-FI 2023 FI-1 00322 Joan Oró).

Author contributions

L.D.S., A.R.M.: Conception and design, creation of the software, analysis and critical interpretation of data, drafting the manuscript. A.G.: Conception and design, creation of the software, analysis and critical interpretation of data, supervision, and substantial revision of

the manuscript. L.G.G., R.F.G., F.V., G.C., R.O.: Acquisition, analysis and interpretation of data, and substantial revision of the manuscript. J.G.O., A.C.P., M.F.C., A.M.G., M.B.A.: analysis and interpretation of data, software updates, and substantial revision of the manuscript. K.M.J., O.W.: interpretation of data, creation of the software, and substantial revision of the manuscript. I.F.G., A.E.: Interpretation of data, supervision, and substantial revision of the manuscript. J.R.P.: Conception and design, interpretation of data, supervision, funding acquisition, and substantial revision of the manuscript. G.T.: Conception and design, analysis and interpretation of data, supervision, funding acquisition, and drafting the original manuscript. All authors read and approved the final manuscript.

Ethics approval and consent

The study was approved by the institutional ethics committee of Vall d'Hebron Hospital (PR(AG)23/2018) on February 16, 2018. All subjects provided written informed consent.

Consent for publication

Not applicable.

Availability of data and materials

The datasets generated and/or analyzed during the current study are not publicly available due to privacy issues but are available from the corresponding author on reasonable request.

Declaration of Competing Interest

The authors declare the following financial interests/personal relationships which may be considered as potential competing interests: Arturo Evangelista and Gisela Teixido-Tura report financial support was provided by Carlos III Health Institute. Jose Rodriguez-Palomares and Ignacio Ferreira Gonzalez report financial support was provided by the Spanish Ministry of Science, Innovation and Universities. Jose Rodriguez-Palomares and Gisela Teixido-Tura report financial support was provided by the Spanish Society of Cardiology. Andrea Guala reports financial support was provided by La Caixa Foundation. Juan Garrido-Oliver reports financial support was provided by Secretaria d'Universitats i Recerca del Departament de Recerca i Universitats de la Generalitat de Catalunya i del Fons Europeu Social Plus. Kevin M. Johnson and Oliver Wieben report a relationship with General Electric Healthcare that includes non-financial support. The other authors declare that they have no known competing financial interests or personal relationships that could have appeared to influence the work reported in this paper.

Acknowledgements

We are grateful to Hannah Cowdrey for the English revision and to Alicia Fresno for all her support.

Appendix A. Supporting information

Supplementary data associated with this article can be found in the online version at doi:10.1016/j.jocmr.2024.101088.

References

[1] Loeys BL, Schwarze U, Holm T, Callewaert BL, Thomas GH, Pannu H, et al. Aneurysm syndromes caused by mutations in the TGF-β receptor. N Engl J Med 2006;355:788–98.
[2] MacCarrick G, Black JH, Bowdin S, El-Hamamsy I, Frischmeyer-Guerrerio PA, Guerrerio AL, et al. Loeys-Dietz syndrome: a primer for diagnosis and management. Genet Med 2014;16:576–87.
[3] Loeys BL, Dietz HC, Braverman AC, Callewaert BL, De Backer J, Devereux RB, et al. The revised Ghent nosology for the Marfan syndrome. J Med Genet 2010;47:476–85.
[4] Faivre L, Collod-Beroud G, Loeys BL, Child A, Binquet C, Gautier E, et al. Effect of mutation type and location on clinical outcome in 1,013 probands with Marfan syndrome or related phenotypes and FBN1 mutations: an international study. Am J Hum Genet 2007;81:454–66.
[5] Vanem TT, Böker T, Sandvik GF, Kirkhus E, Smith HJ, Andersen K, et al. Marfan syndrome: evolving organ manifestations—a 10-year follow-up study. Am J Med Genet Part A 2020;182:397–408.
[6] Milleron O, Arnoult F, Delorme G, Detaint D, Pellenc Q, Raffoul R, et al. Pathogenic FBN1 genetic variation and aortic dissection in patients with Marfan syndrome. J Am Coll Cardiol 2020;75:843–53.
[7] Jondeau G, Detaint D, Tubach F, Arnoult F, Milleron O, Raoux F, et al. Aortic event rate in the Marfan population: a cohort study. Circulation 2012;125:226–32.
[8] Jondeau G, Ropers J, Regalado E, Braverman A, Evangelista A, Teixedo G, et al. International registry of patients carrying TGFBR1 or TGFBR2 mutations: results of the MAC (Montalcino Aortic Consortium). Circ Cardiovasc Genet 2016;9:548–58.
[9] Isselbacher EM, Preventza O, Hamilton Black III J, Augoustides JG, Beck AW, Bolen MA, et al. 2022 ACC/AHA guideline for the diagnosis and management of aortic disease. J Am Coll Cardiol 2022;80:e223–393.
[10] Finkbohner R, Johnston D, Crawford ES, Coselli J, Milewicz DM. Marfan syndrome. Long-term survival and complications after aortic aneurysm repair. Circulation 1995;91:728–33.
[11] Gott VL, Greene PS, Alejo DE, Cameron DE, Naftel DC, Miller DC, et al. Replacement of the aortic root in patients with Marfan's syndrome. N Engl J Med 1999;340:1307–13.
[12] Silverman DI, Burton KJ, Gray J, Bosner MS, Kouchoukos NT, Roman MJ, et al. Life expectancy in the Marfan syndrome. Am J Cardiol 1995;75:157–60.
[13] LeMaire SA, Carter SA, Volguina IV, Laux AT, Milewicz DM, Borsato GW, et al. Spectrum of aortic operations in 300 patients with confirmed or suspected Marfan syndrome. Ann Thorac Surg 2006;81:2063–78.
[14] Patel ND, Arnaoutakis GJ, George TJ, Allen JG, Alejo DE, Dietz HC, et al. Valve-sparing aortic root replacement in Loeys-Dietz syndrome. Ann Thorac Surg 2011;92:556–61.
[15] Martens A, Beckmann E, Kaufeld T, Fleissner F, Neuser J, Korte W, et al. Valve-sparing aortic root replacement (David I procedure) in Marfan disease: single-centre 20-year experience in more than 100 patients. Eur J Cardio-Thorac Surg 2019;55:476–83.
[16] Lenz A, Warncke M, Wright F, Weinrich JM, Schoennagel BP, Henes FO, et al. Longitudinal follow-up by MR angiography reveals progressive dilatation of the distal aorta after aortic root replacement in Marfan syndrome. Eur Radiol 2023;33:6984–92.
[17] Den Hartog AW, Franken R, Zwinderman AH, Timmermans J, Scholte AJ, Van Den Berg MP, et al. The risk for type B aortic dissection in Marfan syndrome. J Am Coll Cardiol 2015;65:246–54.
[18] Weinsaft JW, Devereux RB, Preiss LR, Feher A, Roman MJ, Basson CT, et al. Aortic dissection in patients with genetically mediated aneurysms: incidence and predictors in the GenTAC Registry. J Am Coll Cardiol 2016;67:2744–54.
[19] Roman MJ, Devereux RB, Preiss LR, Asch FM, Eagle KA, Holmes KW, et al. Associations of age and sex with Marfan phenotype: the National Heart, Lung, and Blood Institute GenTAC (Genetically Triggered Thoracic Aortic Aneurysms and Cardiovascular Conditions) Registry. Circ Cardiovasc Genet 2017;10:1–8.
[20] Palumbo MC, Redaelli A, Wingo M, Tak KA, Leonard JR, Kim J, et al. Impact of ascending aortic prosthetic grafts on early postoperative descending aortic biomechanics on cardiac magnetic resonance imaging. Eur J Cardio-Thorac Surg 2022;61:860–8.
[21] Garrido-Oliver J, Aviles J, Mejía-Córdova M, Dux-Santoy L, Ruiz-Muñoz A, Teixidó-Turà G, et al. Machine learning for the automatic assessment of aortic rotational flow and wall shear stress from 4D flow cardiac magnetic resonance imaging. Eur Radiol 2022;32:7117–27.
[22] Johnson KM, Lum DP, Turski PA, Block WF, Mistretta CA, Wieben O. Improved 3D phase contrast MRI with off-resonance corrected dual echo VIPR. Magn Reson Med 2008;60:1329–36.
[23] O'Grady C, Chatzimavroudis GP, Lakkadi NS, Srinivas S, Setser RM. 2088 Effect of spatial resolution on measurement of aortic compliance using MRI. J Cardiovasc Magn Reson 2008;10:A357.
[24] Ruiz-Muñoz A, Guala A, Rodriguez-Palomares J, Dux-Santoy L, Servato L, Lopez-Sainz A, et al. Aortic flow dynamics and stiffness in Loeys–Dietz syndrome patients: a comparison with healthy volunteers and Marfan syndrome patients. Eur Hear J Cardiovasc Imaging 2022;23:641–9.
[25] Dux-Santoy L, Guala A, Teixidó-Turà G, Ruiz-Muñoz A, Maldonado G, Villalva N, et al. Increased rotational flow in the proximal aortic arch is associated with its dilation in bicuspid aortic valve disease. Eur Heart J Cardiovasc Imaging 2019;20:1407–17.
[26] Guala A, Teixido-Tura G, Dux-Santoy L, Granato C, Ruiz-Munõz A, Valente F, et al. Decreased rotational flow and circumferential wall shear stress as early markers of descending aorta dilation in Marfan syndrome: a 4D flow CMR study. J Cardiovasc Magn Reson 2019;21:63.
[27] Rodríguez-Palomares JF, Dux-Santoy L, Guala A, Kale R, Maldonado G, Teixidó-Turà G, et al. Aortic flow patterns and wall shear stress maps by 4D-flow cardiovascular magnetic resonance in the assessment of aortic dilatation in bicuspid aortic valve disease. J Cardiovasc Magn Reson 2018;20:28.
[28] Sotelo J, Dux-Santoy L, Guala A, Rodríguez-Palomares J, Evangelista A, Sing-Long C, et al. 3D axial and circumferential wall shear stress from 4D flow MRI data using a finite element method and a laplacian approach. Magn Reson Med 2018;79:2816–23.
[29] Muñoz AR, Guala A, Cilla M, Martínez M, Dux-Santoy L, Teixidó-Turà G, et al. Aortic stiffness descriptors by cardiac magnetic resonance are correlated with

mechanical testing of ex-vivo aortic aneurysms specimens. Cardiovasc Res 2022;118:cvac157.101.
[30] Guala A, Rodríguez-Palomares JF, Dux-Santoy L, Teixidó-Turà G, Maldonado G, Galian L, et al. Influence of aortic dilation on the regional aortic stiffness of bicuspid aortic valve assessed by 4-dimensional flow cardiac magnetic resonance. Comparison with Marfan syndrome and degenerative aortic aneurysm. J Am Coll Cardiol Imaging 2019;12:1020–9.
[31] Bargiotas I, Mousseaux E, Yu W-C, Venkatesh BA, Bollache E, de Cesare A, et al. Estimation of aortic pulse wave transit time in cardiovascular magnetic resonance using complex wavelet cross-spectrum analysis. J Cardiovasc Magn Reson 2015;17:65.
[32] Guala A, Teixidó-Tura G, Rodríguez-Palomares JF, Ruiz-Muñoz A, Dux-Santoy L, Villalva N, et al. Proximal aorta longitudinal strain predicts aortic root dilation rate and aortic events in Marfan syndrome. Eur Heart J 2019;40:2047–55.
[33] Bianchini E, Lønnebakken MT, Wohlfahrt P, Piskin S, Terentes-Printzios D, Alastruey J, et al. Magnetic resonance imaging and computed tomography for the noninvasive assessment of arterial aging: a review by the VascAgeNet COST action. J Am Heart Assoc 2023;12:e027414.
[34] Semaan E, Markl M, Chris Malaisrie S, Barker A, Allen B, Mccarthy P, et al. Haemodynamic outcome at four-dimensional flow magnetic resonance imaging following valve-sparing aortic root replacement with tricuspid and bicuspid valve morphology. Eur J Cardio-Thorac Surg 2014;45:818–25.
[35] Von Knobelsdorff-Brenkenhoff F, Trauzeddel RF, Barker AJ, Gruettner H, Markl M, Schulz-Menger J. Blood flow characteristics in the ascending aorta after aortic valve replacement - a pilot study using 4D-flow MRI. Int J Cardiol 2014;170:426–33.
[36] Bollache E, Fedak PWM, van Ooij P, Rahman O, Malaisrie SC, McCarthy PM, et al. Perioperative evaluation of regional aortic wall shear stress patterns in patients undergoing aortic valve and/or proximal thoracic aortic replacement. J Thorac Cardiovasc Surg 2018;155:2277–2286.e2.
[37] Sieren MM, Balks MF, Schlueter JK, Wegner F, Huellebrand M, Scharfschwerdt M, et al. Comprehensive analysis of haemodynamics in patients with physiologically curved prostheses of the ascending aorta. Eur J Cardio-Thorac Surg 2022;62:ezab352.
[38] Oechtering TH, Sieren MM, Hunold P, Hennemuth A, Huellebrand M, Scharfschwerdt M, et al. Time-resolved 3-dimensional magnetic resonance phase contrast imaging (4D Flow MRI) reveals altered blood flow patterns in the ascending aorta of patients with valve-sparing aortic root replacement. J Thorac Cardiovasc Surg 2020;159:798–810.e1.
[39] Hope TA, Kvitting JPE, Hope MD, Miller DC, Markl M, Herfkens RJ. Evaluation of Marfan patients status post valve-sparing aortic root replacement with 4D flow. Magn Reson Imaging 2013;31:1479–84.
[40] Calò K, Gallo D, Guala A, Rizzini ML, Dux-Santoy L, Rodriguez-Palomares J, et al. Network-based characterization of blood large-scale coherent motion in the healthy human aorta with 4D flow MRI. IEEE Trans Biomed Eng 2023;70:1095–104.
[41] Calò K, Gallo D, Guala A, Rodriguez Palomares J, Scarsoglio S, Ridolfi L, et al. Combining 4D flow MRI and complex networks theory to characterize the hemodynamic heterogeneity in dilated and non-dilated human ascending aortas. Ann Biomed Eng 2021;49:2441–53.
[42] Collins JD, Semaan E, Barker A, McCarthy PM, Carr JC, Markl M, et al. Comparison of hemodynamics after aortic root replacement using valve-sparing or bioprosthetic valved conduit. Ann Thorac Surg 2015;100:1556–62.
[43] Keller EJ, Malaisrie SC, Kruse J, McCarthy PM, Carr JC, Markl M, et al. Reduction of aberrant aortic haemodynamics following aortic root replacement with a mechanical valved conduit. Inter Cardiovasc Thorac Surg 2016;23:416–23.
[44] Salvi L, Alfonsi J, Grillo A, Pini A, Soranna D, Zambon A, et al. Postoperative and mid-term hemodynamic changes after replacement of the ascending aorta. J Thorac Cardiovasc Surg 2022;163:1283–92.
[45] Palumbo MC, Rong LQ, Kim J, Navid P, Sultana R, Butcher J, et al. Prosthetic aortic graft replacement of the ascending thoracic aorta alters biomechanics of the native descending aorta as assessed by transthoracic echocardiography. PLoS One 2020;15:e0230208.
[46] Dux-Santoy L, Rodríguez-Palomares JF, Teixidó-Turà G, Ruiz-Muñoz A, Casas G, Valente F, et al. Registration-based semi-automatic assessment of aortic diameter growth rate from contrast-enhanced computed tomography outperforms manual quantification. Eur Radiol 2022;32:1997–2009.